PROCEEDINGS OF SPIE

SPIEDigitalLibrary.org/conference-proceedings-of-spie

A new catheter design for combined radiofrequency ablation and optoacoustic treatment monitoring using copper-coated light-guides

Johannes Rebling, Francisco Javier Oyaga Landa, Xosé Luis Deán-Ben, Daniel Razansky

Johannes Rebling, Francisco Javier Oyaga Landa, Xosé Luis Deán-Ben, Daniel Razansky, "A new catheter design for combined radiofrequency ablation and optoacoustic treatment monitoring using copper-coated light-guides," Proc. SPIE 10488, Optical Fibers and Sensors for Medical Diagnostics and Treatment Applications XVIII, 1048805 (13 February 2018); doi: 10.1117/12.2287390



Event: SPIE BiOS, 2018, San Francisco, California, United States

A New Catheter Design for Combined Radiofrequency Ablation and Optoacoustic Treatment Monitoring Using Copper-Coated Light-Guides

Johannes Rebling^{a,b}, Francisco Javier Oyaga Landa^{a,b}, Xosé Luís Deán-Ben^a, Daniel Razansky^{a,b,*}

^aInstitute of Biological and Medical Imaging (IBMI), Helmholtz Center Munich, Ingolstaedter Landstraße 1, 85764 Neuherberg, Germany;

^bSchool of Medicine and School of Bioengineering, Technical University of Munich, Ismaninger Straße 22, 81675 Munich, Germany

ABSTRACT

Electrosurgery, i.e. the application of radiofrequency current for tissue ablation, is a frequently used treatment for many cardiac arrhythmias. Electrophysiological and anatomic mapping, as well as careful radiofrequency power control typically guide the radiofrequency ablation procedure. Despite its widespread application, accurate monitoring of the lesion formation with sufficient spatio-temporal resolution remains challenging with the existing imaging techniques. We present a novel integrated catheter for simultaneous radiofrequency ablation and optoacoustic monitoring of the lesion formation in real time and 3D. The design combines the delivery of both electric current and optoacoustic excitation beam in a single catheter consisting of copper-coated multimode light-guides and its manufacturing is described in detail. The electrical current causes coagulation and desiccation while the excitation light is locally absorbed, generating OA responses from the entire treated volume. The combined ablation-monitoring capabilities were verified using ex-vivo bovine tissue. The formed ablation lesions showed a homogenous coagulation while the ablation was monitored in real-time with a volumetric frame rate of 10 Hz over 150 seconds.

Keywords: cardiac, ablation catheter, photoacoustic, tomography

INTRODUCTION

Radiofrequency catheter ablation (RFA), also known as electro-surgery, helps to eliminate dysfunctional tissue by heating via an alternating radiofrequency (RF) current. It is frequently applied in various fields such as dermatology¹. oncology^{3, 4} and to cure vascular diseases^{5, 6}. Due to reporter higher efficacy rates and lower rates of complications, RFA ablation is the preferred intervention to cure arrhythmias in cardiology⁷⁻⁹. Independent of the application, the clinical outcome of RFA depends strongly on the accurate and timely monitoring of the forming lesion. The outcomes are highly dependent on careful guidance and power control during the procedure and rely mainly on the surgeon's expertise to assess lesion formation, causing large variabilities in the success rates. Ablation procedure are typically guided via electrophysiological and anatomic mapping, as well as careful radiofrequency power titration. Presently, simple and indirect methods of ablation monitoring such as thermal or impedance monitoring are used due to their simplicity. While being simple and cost effective, they suffer from inaccuracy due to slow heat diffusion which often leads to substantial differences between desired and actual lesion size and shape¹⁰⁻¹³. Modern imaging techniques such as intravascular ultrasound (IVUS) and magnetic resonance imaging (MRI) allow precise catheter placement and navigation. MRI further requires a Gadolinium contrast agent to visualize the actual lesion, which only shows a delayed response. This delayed response as well as the restriction to non-magnetic materials and special RF filters for the MRI system make real-time lesion monitoring using MRI very expensive and impractical. IVUS on the other hand offers only a limited view of the tissue with poor spatial resolution and contrast and is hence unable to visualize accurately the actual lesion formation 14-¹⁷. Optical methods aimed at the characterization of RFA in real-time rely on changes in the absorption and emission spectra as the ablated tissue undergoes coagulation and desiccation. Using infrared thermal imaging allows quantification of tissue temperature with high-resolution, but is restricted to superficial imaging. Integrating spectroscopic or optical coherence tomography (OCT) probes into the RF ablation catheter itself enables monitoring of tissue in direct contact with the catheter, but does not provide images of the forming lesion^{18, 19}.

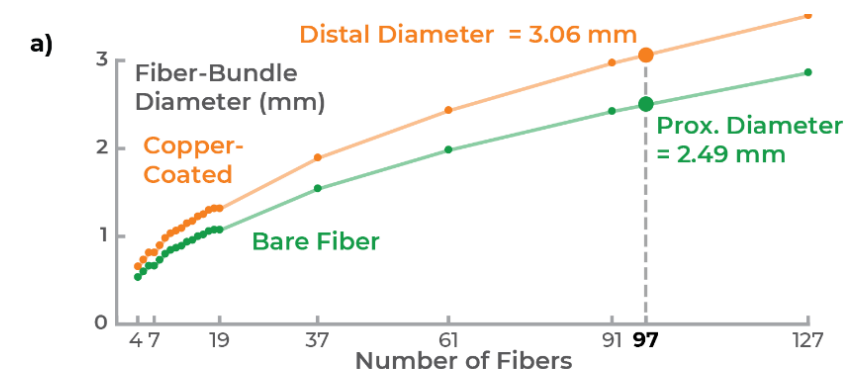
*dr@tum.de, www.razanskylab.org

Optical Fibers and Sensors for Medical Diagnostics and Treatment Applications XVIII, edited by Israel Gannot Proc. of SPIE Vol. 10488, 1048805 · © 2018 SPIE · CCC code: 1605-7422/18/\$18 · doi: 10.1117/12.2287390

Despite its widespread application, accurate monitoring of the lesion formation with sufficient spatio-temporal resolution remains challenging with the existing monitoring techniques. Here we present a combined radiofrequency ablation and optoacoustic imaging (RFOA) catheter. Our unipolar ablation catheter design combines the capability of radiofrequency ablation and light delivery for optoacoustic imaging in a single compact and flexible unit. The catheter design is based on copper-coated light guides, which are bundled, and connectorized to form the RFOA catheter. The manufacturing process of the bundle is described in detail. The RFOA catheter was used to generate ablation lesions of different size in ex-vivo bovine tissue while simultaneously monitoring the lesion formation using OA tomography with the necessary illumination delivered through the RFOA catheter itself.

METHODS

The design of the RFOA catheter is based on copper-coated silica multimode fibers with a core diameter of 200 μ m, a cladding diameter of 220 μ m and a 25 μ m thin copper layer resulting in an overall diameter of 270 μ m. Multimode fibers with a core diameter of 200 μ m of were used as they are easy to process while being flexible enough to be used in a catheter design. The number of fibers in the bundle is limited by both geometry as well as practicability of bundle manufacturing. To this end, the bundle diameter for both bare (220 μ m outer diameter) and copper-coated (270 μ m outer diameter) MMF was calculated for various numbers of fibers in the bundle and assuming optimal packing of the circular fibers within a circular aperture²⁰, as shown in Fig. 1a).



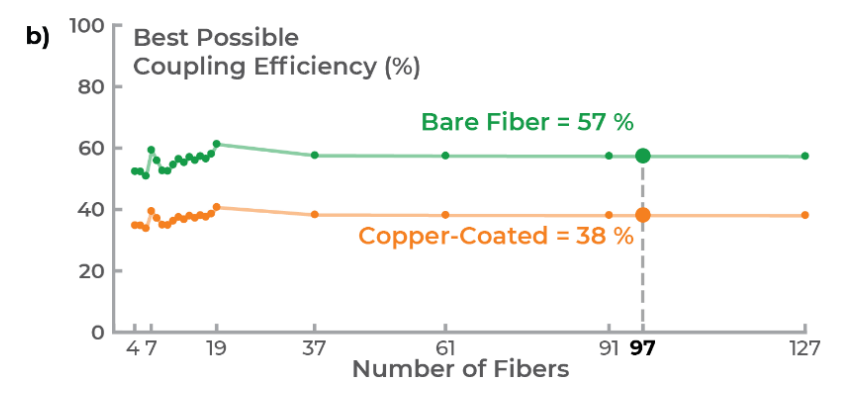


Figure 1. Simulation of fiber-bundle a) diameter and b) theoretical coupling efficiency for both bare and copper-coated multimode fibers.

The bundle was manufactured using 97 individual fibers, which resulted in a bundle diameter of 3.06 mm when optimally packed. The theoretical coupling efficiency (the ratio of light reaching the bundle vs. light exiting the bundle, taking into account the fiber packing ²⁰ as well as a 4% reflections on both facets) shows a poor transmission of light trough the copper coated fibers. This is evident in Fig 2b) where the copper-coated bundle has a theoretical best coupling efficiency of only 38%. This value is not sufficient for an optical bundle, taking into account additional losses due to not-optimal packing and real world optical coupling for the manufactured bundle. The poor coupling efficiency is a result of the large, unused area around the light-conducting core of the MMF. By removing the copper layer at the proximal end, this unused area can be removed drastically. This increases the effective area of the proximal front facet and enhances

the theoretical coupling from 38 % for the copper coated fibers (orange line, Fig. 1b) to 57 % for the bare MMF (green line, Fig. 1b). Removing the copper also reduced the effective bundle diameter from 3.06 mm to 2.49 mm as shown in Fig. 1a).

Figure 2 shows the step-by-step manufacturing of the combined RF ablation and OA imaging catheter. The individual fibers were cut to a length of approximately 1.5 m and were combined to form a bundle of sufficient size to create RF lesions and to transport a sufficient amount of light to allow effective optoacoustic monitoring of the forming lesion, as shown in Fig. 1a). The copper coating of the distal end of the bundle was removed over a length of approximately 20 cm, using an acidic solution of iron(III) chloride, which selectively etched the copper in less than 10 minutes, as shown in Fig. 1b). The proximal, copper-free end of the bundle was glued into a conventional, stainless steel SMA905 MMF connector²¹, where the central bore was increased from 1.5 mm to 2.6 mm to accommodate the bundle, as shown in Fig. 2c). The distal end of the bundle was connectorized using a customized stainless steel ferule with a 4 mm central bore. Both the proximal and distal ends were glued using high temperature epoxy²² and cured at 80°C for 30 minutes. Both facets were manually polished to optical quality using conventional polishing/lapping film down to a grit size of 0.3μm²³. The polished facets are shown in Fig. 2d). The RF connection cable was then soldered to the bundle near the proximal end the assembled bundle was protected and insulated using PVC tubing, as shown in Fig. 2e). Figure 2e) shows the fully assembled bundle.

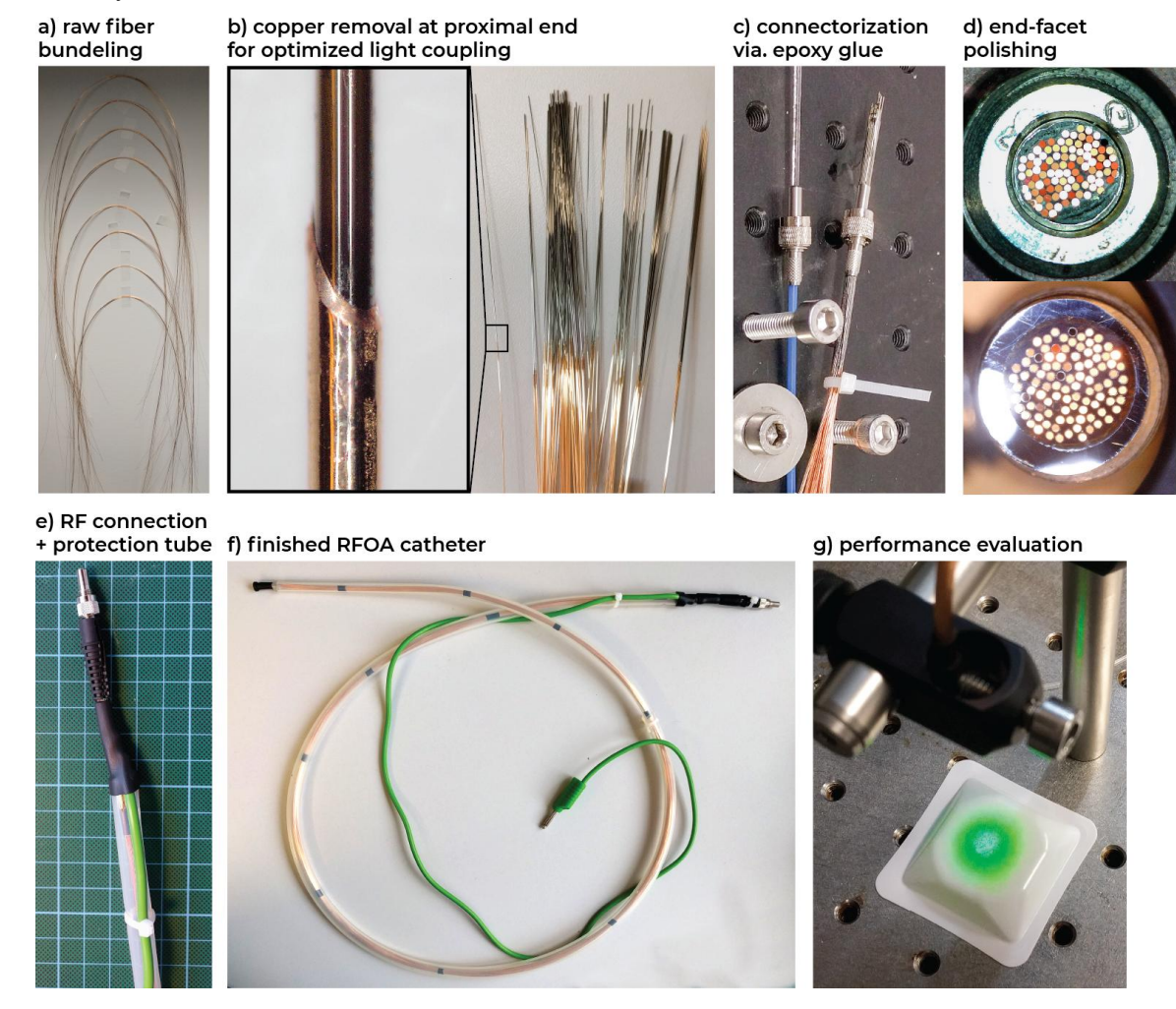


Figure 2. Step-by-step manufacturing of the combined RF ablation and OA imaging catheter. a) Single, copper-coated multimode fibers were cut to a length of approximately 1.5 m and were combined to form a bundle. b) The copper coating was removed at the proximal end of the bundle to achieve a better coupling efficiency. c) and d) Both the proximal and distal ends were connectorized using high-temperature epoxy glue and were subsequently polished. e) The RF cable was soldered to the bundle near the proximal end the assembled bundle was protected and insulated using PVC tubing. f) Fully assembled bundle. g) Uniform light delivery trough the bundle.

The experimental setup used to demonstrate simultaneous RF ablation and OA imaging is shown in Fig. 3. The OA imaging setup is based on a spherical, high-frequency ultrasound matrix that is used in combination with a tunable, pulsed OPO laser. A detailed description of the system and its performance can be found elsewhere²⁴. The light of the OPO (780 nm, 5 ns pulses) is coupled into the proximal end of the RFOA catheter via a simple lens (f=50 mm) and with the bundles SMA MMF connector fixed on the optical table to allow stable coupling. The light exists the bundle at the distal end where it is locally absorbed in the tissue sample. The absorbed energy generates high frequency optoacoustic signals, which propagate trough the tissue and the surrounding water and are detected by a 512-element ultrasound matrix array. The signals are digitized and a volumetric image is reconstructed in real-time using a GPU-based reconstruction algorithm²⁵. The RF signal is generated in a custom build RF generator that delivers 20 kHz ablation current with a duty-cycle of 3%. The signal was coupled to the RFOA bundle via the soldered RF cable and ground was provided via a large-area pad in the water (not shown). The solder spot connects the RF cable to all individual strains of the RFOA bundle, thus evenly distributing the current at the output facet over the whole area of the ablation tip.

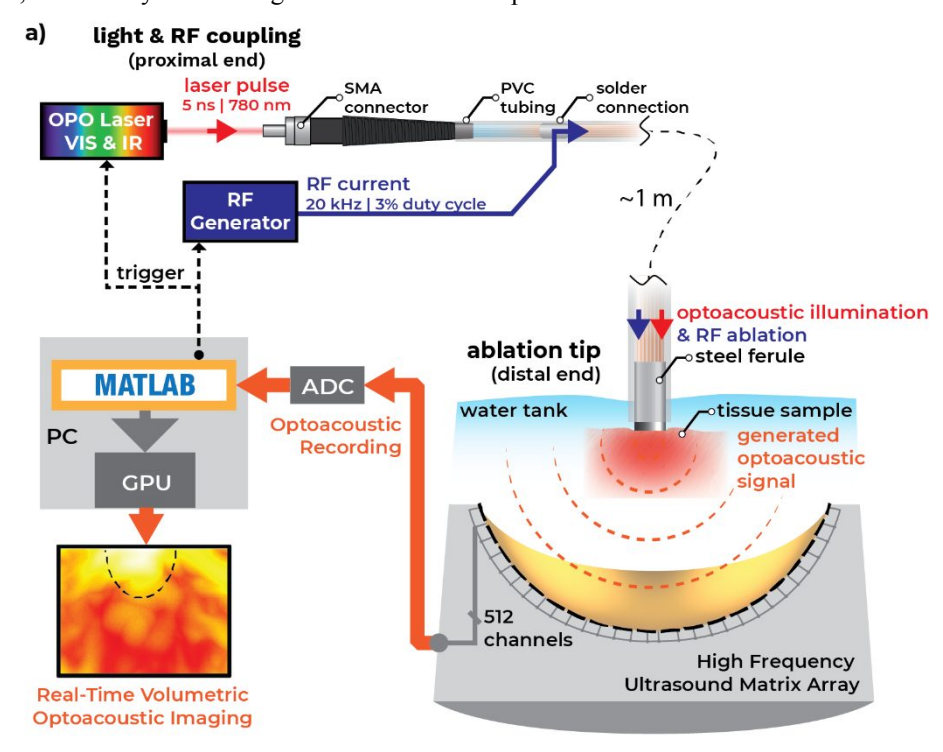


Figure 3. Schematic of the simultaneous radiofrequency ablation and optoacoustic imaging setup.

RESULTS & DISCUSSION

Figure 2e) shows the uniform and intense light distribution exiting the distal end of the RFOA bundle. A coupling efficiency of approximately 50% was achieved, which is close to the theoretically optimal value of 57%. The theoretical coupling efficiency was not achieved due to a sub-optimal packing of the fibers, as evident in Fig. 2d). However, a perpulse energy of 6 mJ was transferred trough the bundle without visible damage to the proximal end facet, which is sufficient for OA tomography. The electrical resistance between the distal steel ferule and the input of the RF cable was less than 5 Ω , showcasing the excellent conductivity of the RFOA bundle due to the thick diameter and the multiple copper coated fibers.

The RFOA bundle was then used to ablate a bovine tissue sample while simultaneously monitoring the progressing lesion in real time, as shown in Fig. 4. The tissue was ablated for 30 seconds and OA monitoring was perform at an

imaging rate of 10 Hz for a total of 150 seconds. OA images are normalized to the baseline prior to the start of the ablation and hence show the relative change in the OA signal. Figure 4a) show exemplary slices through the center of the volumetric OA images at the start (t = 0 s), and for every 10 seconds at t = 10, 20 and 30 s as well as after tissue cooling at t = 150s. A strong increase of the OA signal is visible after just 10 seconds and increases further towards the end of the ablation at t = 30 s. The formed lesion is shown in Figure 4b), with a top view of the lesion shown on the left and a slice through the tissue sample is shown on the right. Both the top and side view show a white coagulum that penetrates approximately 2-4 mm into the tissue from the point of contact with the ablation tip. No charring is visible and the lesions is symmetric and uniform.

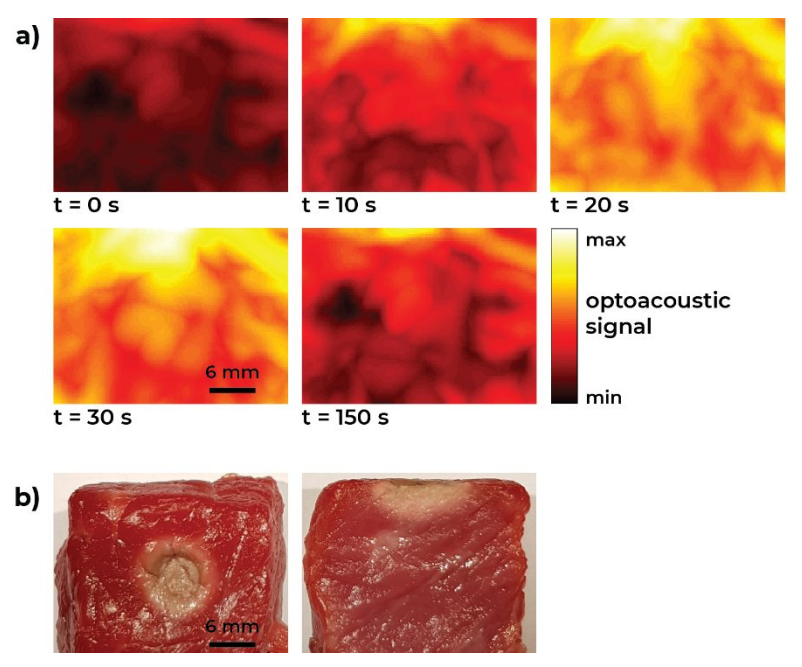


Figure 4. Simultaneous radiofrequency ablation and optoacoustic monitoring using the RFOA catheter. The forming lesion was imaged in real-time and the formed coagulum is uniform and symmetric without visible charring.

ACKNOWLEDGMENTS

This work was supported by the German Research Foundation (DFG) Grant RA 1848/5-1 and by the European Union through the OILTEBIA (Optical Imaging and Laser Techniques for Biomedical Applications) ITN, Grant Agreement No. 317526.

REFERENCES

- [1] S. Sachdeva, and A. Dogra, "Radiofrequency ablation in dermatology," Indian Journal of Dermatology, 52(3), 134 (2007).
- [2] D. H. Kim, D. J. Hyun, R. Piquette, C. Beaumont, L. Germain, and D. Larouche, "27.12 MHz Radiofrequency Ablation for Benign Cutaneous Lesions," BioMed research international, 2016, (2016).
- [3] M.-H. Chen, W. Yang, K. Yan, M.-W. Zou, L. Solbiati, J.-B. Liu, and Y. Dai, "Large liver tumors: protocol for radiofrequency ablation and its clinical application in 110 patients—mathematic model, overlapping mode, and electrode placement process," Radiology, 232(1), 260-271 (2004).
- [4] S. L. Wong, P. B. Mangu, M. A. Choti, T. S. Crocenzi, G. D. Dodd III, G. S. Dorfman, C. Eng, Y. Fong, A. F. Giusti, and D. Lu, "American Society of Clinical Oncology 2009 clinical evidence review on radiofrequency ablation of hepatic metastases from colorectal cancer," Journal of Clinical Oncology, 28(3), 493-508 (2009).

- [5] C. V. Chandrasekaran, Z. Guo, A. J. Pantages, D. Masters, and R. Kaveckis, [RF ablation and ultrasound catheter for crossing chronic total occlusions] Google Patents, (2002).
- [6] G. Munger, A. Pandey, and R. Viswanathan, [Method and Apparatus for Ablative Recanalization of Blocked Vasculature] Google Patents, (2008).
- [7] S. K. S. Huang, "Catheter Ablation of Cardiac Arrhythmias," Saunders, (2014).
- [8] T. Terasawa, E. M. Balk, M. Chung, A. C. Garlitski, A. A. Alsheikh-Ali, J. Lau, and S. Ip, "Systematic review: comparative effectiveness of radiofrequency catheter ablation for atrial fibrillation," Ann Intern Med, 151(3), 191-202 (2009).
- [9] S. S. Yu, W. D. Tope, and R. C. Grekin, "Cardiac devices and electromagnetic interference revisited: new radiofrequency technologies and implications for dermatologic surgery," Dermatol Surg, 31(8 Pt 1), 932-40 (2005).
- [10] D. E. Haines, "The biophysics of radiofrequency catheter ablation in the heart: the importance of temperature monitoring," Pacing and Clinical Electrophysiology, 16(3), 586-591 (1993).
- [11] J. J. Langberg, H. Calkins, R. El-Atassi, M. Borganelli, A. Leon, S. J. Kalbfleisch, and F. Morady, "Temperature monitoring during radiofrequency catheter ablation of accessory pathways," Circulation, 86(5), 1469-1474 (1992).
- [12] M. Harvey, Y. N. Kim, J. Sousa, R. el-Atassi, F. Morady, H. Calkins, and J. J. Langberg, "Impedance monitoring during radiofrequency catheter ablation in humans," Pacing Clin Electrophysiol, 15(1), 22-7 (1992).
- [13] I. D. McRury, D. Panescu, M. A. Mitchell, and D. E. Haines, "Nonuniform heating during radiofrequency catheter ablation with long electrodes: monitoring the edge effect," Circulation, 96(11), 4057-64 (1997).
- [14] M. Wright, E. Harks, S. Deladi, F. Suijver, M. Barley, A. van Dusschoten, S. Fokkenrood, F. Zuo, F. Sacher, M. Hocini, M. Haissaguerre, and P. Jais, "Real-time lesion assessment using a novel combined ultrasound and radiofrequency ablation catheter," Heart Rhythm, 8(2), 304-12 (2011).
- [15] C. Y. Wang, X. Geng, T. S. Yeh, H. L. Liu, and P. H. Tsui, "Monitoring radiofrequency ablation with ultrasound Nakagami imaging," Med Phys, 40(7), 072901 (2013).
- [16] G. R. Vergara, S. Vijayakumar, E. G. Kholmovski, J. J. Blauer, M. A. Guttman, C. Gloschat, G. Payne, K. Vij, N. W. Akoum, M. Daccarett, C. J. McGann, R. S. Macleod, and N. F. Marrouche, "Real-time magnetic resonance imaging-guided radiofrequency atrial ablation and visualization of lesion formation at 3 Tesla," Heart Rhythm, 8(2), 295-303 (2011).
- [17] C. J. McGann, E. G. Kholmovski, R. S. Oakes, J. J. Blauer, M. Daccarett, N. Segerson, K. J. Airey, N. Akoum, E. Fish, T. J. Badger, E. V. DiBella, D. Parker, R. S. MacLeod, and N. F. Marrouche, "New magnetic resonance imaging-based method for defining the extent of left atrial wall injury after the ablation of atrial fibrillation," J Am Coll Cardiol, 52(15), 1263-71 (2008).
- [18] L. M. Epstein, M. A. Mitchell, T. W. Smith, and D. E. Haines, "Comparative study of fluoroscopy and intracardiac echocardiographic guidance for the creation of linear atrial lesions," Circulation, 98(17), 1796-801 (1998).
- [19] R. P. Singh-Moon, C. C. Marboe, and C. P. Hendon, "Near-infrared spectroscopy integrated catheter for characterization of myocardial tissues: preliminary demonstrations to radiofrequency ablation therapy for atrial fibrillation," Biomed Opt Express, 6(7), 2494-511 (2015).
- [20] E. Specht, [The best known packings of equal circles in a circle], http://www.packomania.com/(2016).
- [21] THORLABS, [1580µm SMA CONNECTOR], https://www.thorlabs.de/drawings/3a9f93e71ff5aab5-2645DF38-F8A6-A404-7F97F1C22C8F964B/11580A-AutoCADPDF.pdf(2015).
- [22] I. Epoxy Technology, [EPO-TEK 353ND], https://www.thorlabs.de/drawings/3a9f93e71ff5aab5-2645DF38-F8A6-A404-7F97F1C22C8F964B/353NDPK-MFGSpec.pdf.
- [23] THORLABS, [FN96A Guide to Connectorization and Polishing Optical Fibers], https://www.thorlabs.de/drawings/f96d1cb29825cb7b-C4D6788B-F29E-8F8A-D8FFB5A456BC9E31/FN96A-Manual.pdf (2015).
- [24] X. Luís Deán-Ben, and D. Razansky, "Adding fifth dimension to optoacoustic imaging: volumetric time-resolved spectrally enriched tomography," Light: Science & Applications, 3(1), (2014).
- [25] X. L. Dean-Ben, A. Ozbek, and D. Razansky, "Volumetric real-time tracking of peripheral human vasculature with GPU-accelerated three-dimensional optoacoustic tomography," IEEE Trans Med Imaging, 32(11), 2050-5 (2013).